Received: 23 January 2019 | Revised: 11 June 2019 | Accepted: 19 October 2019

DOI: 10.1111/cmi.13136

WILEY

RESEARCH ARTICLE

The chlamydial deubiquitinase Cdu1 supports recruitment of Golgi vesicles to the inclusion

Daniela Auer[1] | Sophie D. Hügelschäffer[1] | Annette B. Fischer[1] | Thomas Rudel[1,2]

[1]Department of Microbiology, University of Wuerzburg Biocenter, Wuerzburg, Germany

[2]Helmholtz Institute for RNA-based Infection Research (HIRI), Würzburg, Germany

Correspondence
Thomas Rudel, Department of Microbiology, University of Wuerzburg Biocenter, Am Hubland, 97074 Wuerzburg, Germany.
Email: thomas.rudel@biozentrum.uni-wuerzburg.de

Funding information
Deutsche Forschungsgemeinschaft, Grant/Award Number: GRK 2243 Understanding Ubiquitylation: From Molecular Mechanisms to Disease

Abstract

Chlamydia trachomatis is the main cause of sexually transmitted diseases worldwide. As obligate intracellular bacteria *Chlamydia* replicate in a membrane bound vacuole called inclusion and acquire nutrients for growth and replication from their host cells. However, like all intracellular bacteria, *Chlamydia* have to prevent eradication by the host's cell autonomous system. The chlamydial deubiquitinase Cdu1 is secreted into the inclusion membrane, facing the host cell cytosol where it deubiquitinates cellular proteins. Here we show that inactivation of Cdu1 causes a growth defect of *C. trachomatis* in primary cells. Moreover, ubiquitin and several autophagy receptors are recruited to the inclusion membrane of Cdu1-deficient *Chlamydia*. Interestingly, the growth defect of *cdu1* mutants is not rescued when autophagy is prevented. We find reduced recruitment of Golgi vesicles to the inclusion of *Cdu1* mutants indicating that vesicular trafficking is altered in bacteria without active deubiquitinase (DUB). Our work elucidates an important role of Cdu1 in the functional preservation of the chlamydial inclusion surface.

KEYWORDS

autophagy, Cdu1, ChlaDUB1, *Chlamydia trachomatis*, DUB, Golgi, xenophagy

1 | INTRODUCTION

Chlamydia trachomatis is an obligate intracellular human pathogen and the most common transmitted sexually disease worldwide (Newman et al., 2015). Infection with the pathogen can manifest in a spectrum of diseases like ectopic pregnancy, infertility but also in the blinding eye disease trachoma (Bartlett, Levison, & Munday, 2013; Bébéar & de Barbeyrac, 2009; Wright, Turner, & Taylor, 2008). *Chlamydia* replicate in a biphasic developmental cycle. Chlamydial elementary bodies (EBs) infect epithelial cells via the endocytotic pathway and transform into replicative reticulate bodies (RBs) within a vacuole, the chlamydial inclusion (Engel, 2004). After several rounds of replication inside the inclusion, RBs complete their life cycle and transform back into infectious EBs which are released from the host cell via extrusion or cell lysis (Hybiske & Stephens, 2007). *Chlamydia* secrete several effectors into the host cell by the type III secretion system (Subtil et al., 2005; Valdivia, 2008) to orchestrate their developmental cycle, receive host cell metabolites and prevent damage or premature death of their host cell. The natural ribbon-like Golgi architecture is destroyed in cells infected with *C. trachomatis* and vesicular mini stacks originating from fragmented Golgi closely associate with the chlamydial inclusion (Heuer et al., 2009). Host cell sphingolipids are required for the intracellular growth of *C. trachomatis* in epithelial cells, with sphingomyelin attained via the intersection of the chlamydial inclusion with these Golgi-derived vesicles (Hackstadt, Rockey, Heinzen, & Scidmore, 1996).

As all pathogenic bacteria, *Chlamydia* has to subvert the host's immune system to establish a successful infection and both, the adaptive and the innate immune response are effective to control chlamydial infections (Fischer & Rudel, 2016). The cell autonomous immune defence present in all human cells is particularly relevant for an obligate

Daniela Auer and Sophie D. Hügelschäffer contributed equally to this work.

intracellular pathogen like *Chlamydia* (Fischer & Rudel, 2016). A very efficient arm of cell autonomous defence is the removal of pathogens via autophagy. Foreign particles like intracellular bacteria in the cytosol or in vacuoles are specifically marked by ubiquitination. In eukaryotic cells poly-ubiquitination of proteins via lysine 63 (K63) is mainly involved in autophagic events like mitophagy or the removal of *Salmonella* from the cytoplasma via xenophagy, a form of autophagy specifically targeting bacteria (Geisler et al., 2010; Van Wijk et al., 2012).

K48 poly-ubiquitination of proteins often serves as a signal for proteasomal degradation (Hershko & Ciechanover, 1998; Vucic, Dixit, & Wertz, 2011). Ubiquitination of any kind happens via a cascade of several proteins (Kleiger & Mayor, 2014). This posttranslational modification is tightly regulated but also reversible by removal of the ubiquitin by deubiquitinating enzymes (DUBs).

Ubiquitination of the bacterial membrane or the surrounding vacuole membrane then recruits autophagy adapter proteins to the ubiquitin molecules (Kirkin, Lamark, Johansen, & Dikic, 2009; Svenning & Johansen, 2013). As a consequence, ubiquitin bound adapters recruit autophagy-related gene 8 (ATG8) family proteins like the light chain 3 (LC3) protein which mediate the formation of the autophagosome around the intruder. Finally, autophagosomes fuse with lysosomes resulting in the destruction of the engulfed bacteria in the formed autolysosomes (Dikic, 2017).

However, bacteria have evolved strategies to interfere with the autophagy system in order to stay alive and proliferate. In *Salmonella* infection one third of all bacteria are targeted for lysosomal degradation through xenophagy (Birmingham, Smith, Bakowski, Yoshimori, & Brumell, 2006). This affects free *Salmonella* in the host cytosol as well as bacteria engulfed in the *Salmonella* containing vacuole (SCV). The SCV membrane often gets punctured which leads to the recruitment of the autophagy system (Thurston, Wandel, von Muhlinen, Foeglein, & Randow, 2012). In order to prevent clearance *Salmonella* has evolved mechanisms to repair the damaged SCV (Kreibich et al., 2015). Moreover, *Salmonella* secrete SopA into the cytosol, a HECT E3 ligase with yet unknown targets (Zhang, Higashide, McCormick, Chen, & Zhou, 2006). Also *Legionella*, *E. coli* and *Shigella* are known to secrete effector proteins into the host cell that interfere with the ubiquitination system, often by mimicking E3 ligases (Huibregtse & Rohde, 2014). *Chlamydia* has also established mechanisms to evade autophagosomal degradation. Early studies revealed that *C. trachomatis* inclusions do not fuse with autophagosomes in human epithelial cells (Al-Younes, Brinkmann, & Meyer, 2004). The adaptation of *Chlamydia* species to the host specific autophagy system is a fascinating example of co-evolution. The mouse pathogen *C. muridarum* was able to overcome autophagic defence in mouse cells, whereas the human pathogen *C. trachomatis* was susceptible (Yasir, Pachikara, Bao, Pan, & Fan, 2011). In human epithelial cells, in contrast, *C. muridarum* inclusions attracted several components of the autophagy pathway. However, *C. trachomatis* inclusions were resistant to ubiquitination, which prevented the association of the autophagy adaptors p62 and nuclear dot protein 52 kDa (NDP52) and the autophagosomal marker LC3 with the inclusion (Haldar et al., 2016).

Although the chlamydial factors mediating the evasion of host autophagy remain unknown, *Chlamydia* appears to subvert host autophagy by at least two mechanisms: (a) keeping the inclusion intact (Weber et al., 2017b); and (b) interfering with initial ubiquitination of the inclusion. The genome of *C. trachomatis* encodes for two deubiquitinases *Chla*DUB1 and *Chla*DUB2, hereafter referred to as Cdu1 and Cdu2 (Misaghi et al., 2006). We recently showed that Cdu1 is secreted into the chlamydial inclusion facing with its active site to the host cell cytoplasm where it interacts with the host cell proteome and stabilises anti-apoptotic Mcl-1 through deubiquitination (Fischer et al., 2017).

In this paper we show that Cdu1 is essential for normal development in primary host cells. Inactivation of Cdu1 in *Chlamydia* resulted in the recruitment of the autophagy machinery to and phagophore formation at the chlamydial inclusion. Despite phagophore formation at the *cdu1* mutant inclusion, autophagy was not effective in interfering with chlamydial development. The lack of active Cdu1 prevents Golgi vesicle recruitment and slows the transition of RB to EB resulting in decreasing progeny.

2 | RESULTS

2.1 | *Chlamydia* require Cdu1 for growth in primary cells

We previously demonstrated that a transposon insertion mutant of *cdu1* (*Ctr* Tn-*cdu1*) expressing truncated Cdu1 protein is attenuated in a mouse infection model and in cell lines challenged with interferon-γ (IFN-γ) (Fischer et al., 2017). In the absence of IFN-γ *Ctr* Tn-*cdu1* grew without significant difference in several tumour cell lines (Fischer et al., 2017). Tumour cell lines are known to have altered cell autonomous defence including autophagy (Kimmelman, 2011). We therefore asked whether primary cells permit the development of *Ctr* Tn-*cdu1* like previously observed for tumour cells. Primary human fallopian tube cells (Fimb) and human umbilical vein endothelial cells (HUVEC) were infected with wild-type and mutant bacteria and the relative infectivity was determined by transferring bacteria after 48 hr from these primary infections to fresh cells (here referred to as infectivity assay). Fimb and HUVEC infected with *Ctr* Tn-*cdu1* produced less infectious chlamydial particles compared to wild-type infected cells (Figure 1a). In contrast, no deficiency in growth was detected in tumour cell lines like HeLa under these conditions. A detailed analysis of later infection time points revealed a delayed development of *Ctr* Tn-*cdu1* compared to wild-type bacteria (Figure 1b). Moreover, electron microscopy (EM) pictures revealed that *Ctr* Tn-*cdu1* inclusions in Fimb cells harbour less chlamydial particles 30 hr post infection than wild-type *Chlamydia* (Figure 1c, d). The ratio of EBs in *Ctr* Tn-*cdu1* infected cell was reduced compared to wild-type *Chlamydia* (Figure 1d). Therefore, the transition of RB to EB seems to be stalled in the mutant infection. The differentiation of RB to EB is not completely understood, nevertheless, the size of RBs is discussed to be important in this process (Lee et al., 2018). We measured the average size of RBs in chlamydial inclusions after 30 hr in Fimb cells and found that RBs of wild-type *Chlamydia* were significantly smaller

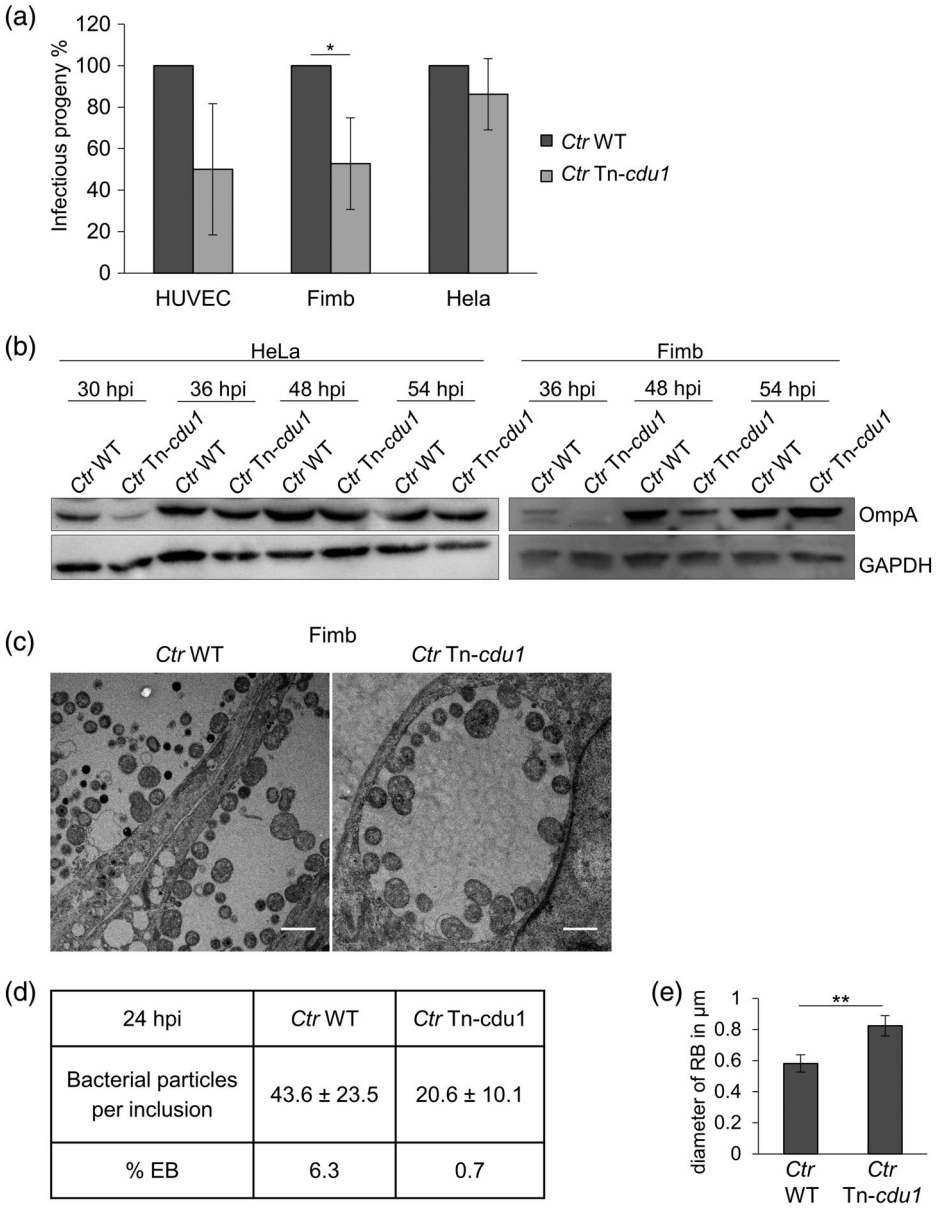

24 hpi	*Ctr* WT	*Ctr* Tn-cdu1
Bacterial particles per inclusion	43.6 ± 23.5	20.6 ± 10.1
% EB	6.3	0.7

FIGURE 1 Inactive Cdu1 results in reduced bacterial growth in primary cells. (a) Primary HUVEC and Fimb and HeLa cells were infected with *Ctr* WT (wild-type) or *Ctr* Tn-*cdu1* at a multiplicity of infection (MOI) of 0.3 for primary cells and a MOI of 1 for HeLa cells. Lysates of primary infected cells were prepared after 24 hr. For progeny infection lysates were taken 48 hpi and used to infect fresh cells (see Experimental procedures for details). Twenty four hours later, lysates of these cells were investigated by Western blotting. Shown is the relative amount of chlamydial HSP60 (cHSP60) or OmpA. Protein loading was normalised to actin. Significance was calculated with the Student's *t* test. **p* < .05, HeLa, HUVEC *n* = 3, Fimb *n* = 4. (b) Fimb and HeLa cells were infected with *Ctr* WT or *Ctr* Tn-*cdu1* at MOI 0.3 and MOI 1 respectively. At indicated time points post infection, infected cells were lysed and the supernatant was used to infect fresh cells. Twenty four hours later, cells were lysed in sodium dodecyl sulfate (SDS)-sample buffer and chlamydial load was determined by immunoblot for OmpA. GAPDH was used as a loading control. (c) Fimb cells were infected with *Ctr* WT or *Ctr* Tn-*cdu1* with a MOI of 0.3. 30 hpi cells were fixed and prepared for EM (see Experimental procedures for details). Scale bar, 1 µm. (d) Quantification of bacterial particles, reticulate bodies (RBs) and elementary bodies (EBs) in Fimb cells infected with *Ctr* WT or *Ctr* Tn-*cdu1* for 24 hr using EM pictures. Infection and samples preparation for EM was done as described in (b). Bacterial particles of 22 inclusions were analysed. (e) Fimb cells were infected with *Ctr* WT or *Ctr* Tn-*cdu1* MOI 0.3 for 30 hr. Cells were fixed and prepared for EM. Transmission electron microscopy pictures were taken and RB diameter from five inclusions for each sample was measured. Significance was calculated with the Student's *t* test. ** *p* < .01

(0.5814 µm ± 0.056) than RBs of the bacteria lacking an active Cdu1 deubiquitinase (0.8236 µm ± 0.065) (Figure 1e). Thus, *Chlamydia* lacking active Cdu1 are developing slower, resulting in less infectious EBs compared to the wild-type bacteria.

2.2 | Inclusions of *Ctr* Tn-*cdu1* are ubiquitinated

Recently we showed that the deubiquitinase Cdu1 is secreted into the inclusion membrane with the active site located on the host cell

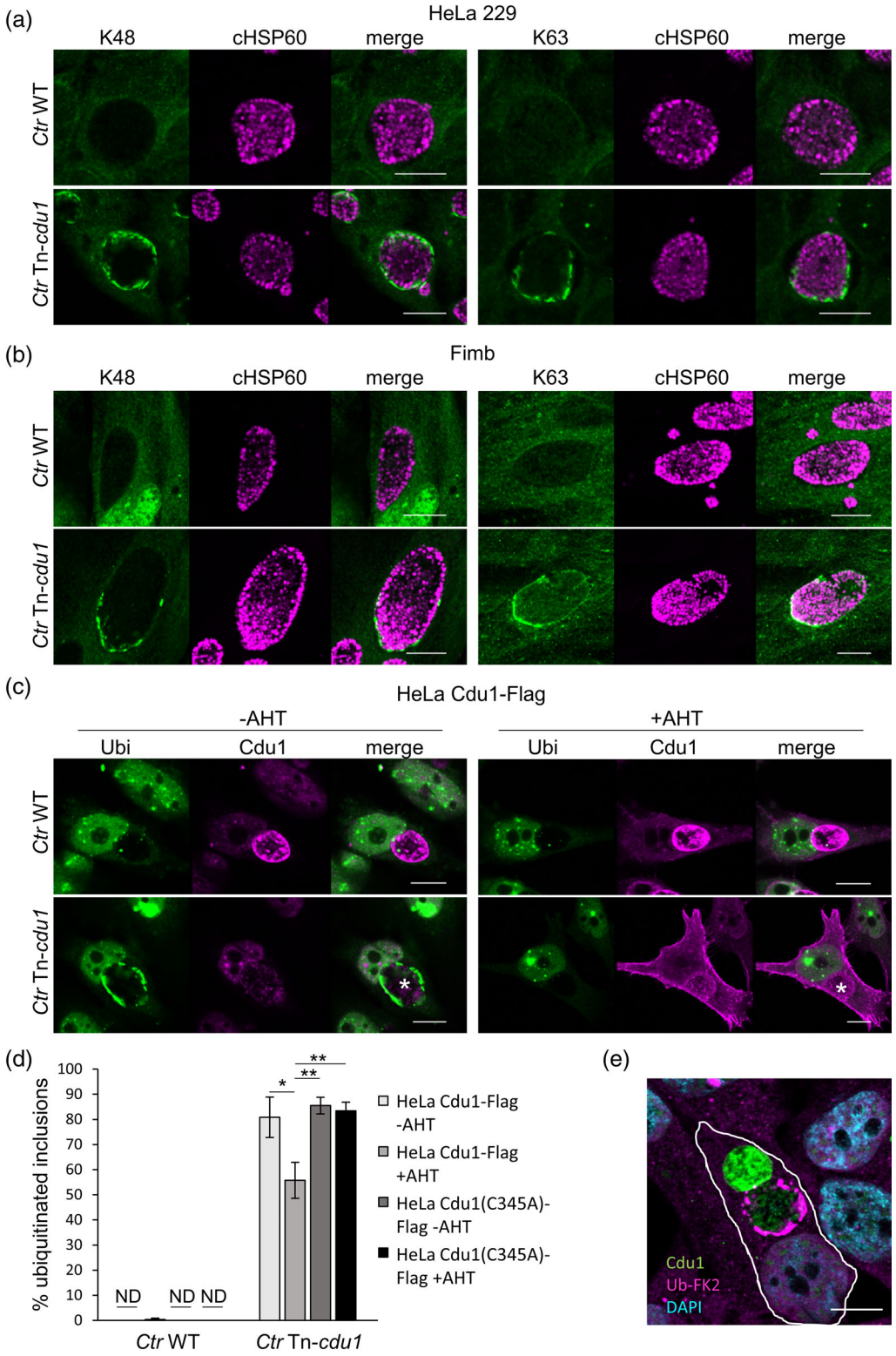

FIGURE 2 *Ctr* Tn-*cdu1* inclusion is ubiquitinated. HeLa (a) or Fimb cells (b) were infected with *Ctr* WT or *Ctr* Tn-*cdu1* for 24 hr at a MOI of 1 or 0.3 respectively. Cells were fixed with 4% paraformaldehyde (PFA)/sucrose followed by indirect immunofluorescence. Chlamydial HSP60 (pink) as well as K48-linked ubiquitin (green, left panel) or K63-linked ubiquitin (green, right panel) was detected. Scale bar, 10 μm. (c) Hela Cdu1-Flag cells were infected with *Ctr* WT or *Ctr* Tn-*cdu1* at a MOI of 1 for 24 hr with/without addition of AHT (50 ng/ml) for 4 hr. Cells were fixed with 4% PFA/sucrose and indirect immunofluorescence was performed with ubiquitin (green) and Cdu1 (pink). The asterisk shows the chlamydial inclusion. Scale bar, 10 μm. (d) Quantification of (c) showing ubiquitination of *Ctr* WT or *Ctr* Tn-*cdu1* inclusions in HeLa Cdu1-Flag and HeLa Cdu1(C345A)-Flag cells upon AHT treatment. Pictures shown in (c) from three independent experiments were used to count 100 inclusions per replicate with and without ubiquitin signal around the chlamydial inclusion. ND, not detected. (e) HeLa cells were infected with *Ctr* WT and *Ctr* Tn-*cdu1* at a MOI of 1 for 24 hr before cells were fixed using 4% PFA/sucrose. Indirect immunofluorescence was performed against Cdu1 (green), ubiquitin (pink) and 4′,6-Diamidino-2-phenylindol (DAPI) for DNA (blue). Cell contours are marked in white. Scale bar, 10 μm

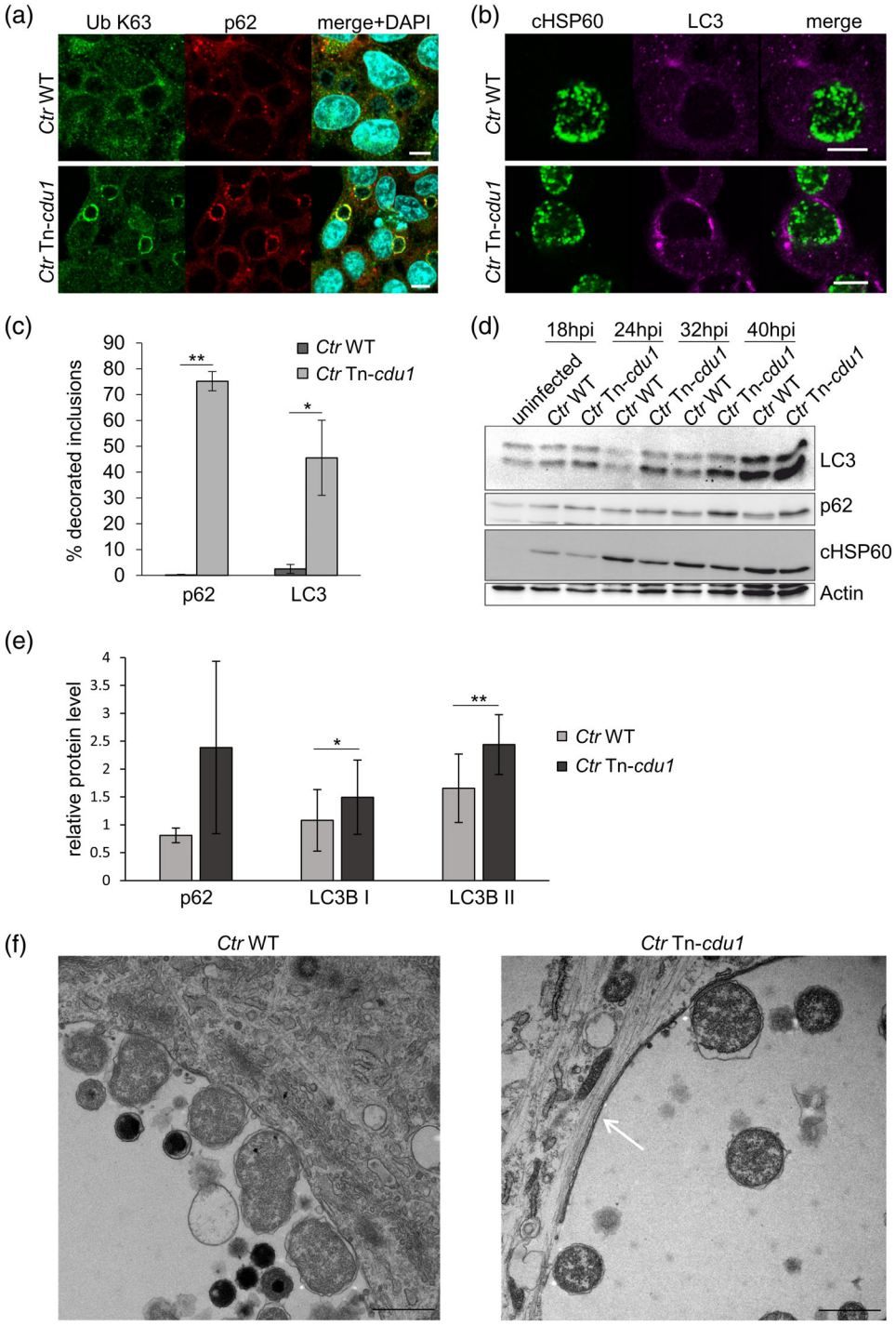

FIGURE 3 Ubiquitinated inclusions of *Ctr* Tn-*cdu1* are recognised by the host cell autophagy system. (a) HeLa cells were infected with *Ctr* WT or *Ctr* Tn-*cdu1* at a MOI of 1 for 24 hr. Cells were fixed with 4% PFA/sucrose and indirect immunofluorescence microscopy was performed with K63 ubiquitin (green), p62/SQSTM1 (red) and DAPI for DNA. Scale bar, 10 μm. (b) HeLa cells were infected with the chlamydial strains *Ctr* WT and *Ctr* Tn-*cdu1* at a MOI of 1 for 24 hr followed by fixation with 4% PFA/sucrose. For indirect immunofluorescence microscopy cells were stained for cHSP60 (green) and light chain 3 (LC3) (pink). Scale bar, 10 μm. (c) Immunofluorescence images of *Ctr* WT and *Ctr* Tn-*cdu1* infected HeLa cells were analysed by counting inclusions positive for p62 or LC3 recruitment. 34 pictures of three independent experiments were counted. Significance was calculated by Student's *t* test. * $p < .05$, ** $p < .001$. (d) HeLa cells were infected with *Ctr* WT or *Ctr* Tn-*cdu1* at a MOI of 1 for the indicated time points. Cells were then lysed in SDS-sample buffer and expression of p62, LC3, cHSP60 and beta-Actin was detected by immunoblot. (e) The levels of the indicated proteins from the immunoblots shown in panel (d) were quantified for the 24 hpi time point. Shown are the mean from three independent experiments ±*SD*. Significance was tested using the Student's *t* test. * $p \leq .05$, ** $p \leq .01$. (f) Fimb cells infected with *Ctr* WT or *Ctr* Tn-*cdu1* at a MOI of 0.3 for 30 hr were fixed for EM preparation. Representative images are shown. The white arrow appoints to a double membrane forming around the chlamydial inclusion. Scale bar, 1 μm

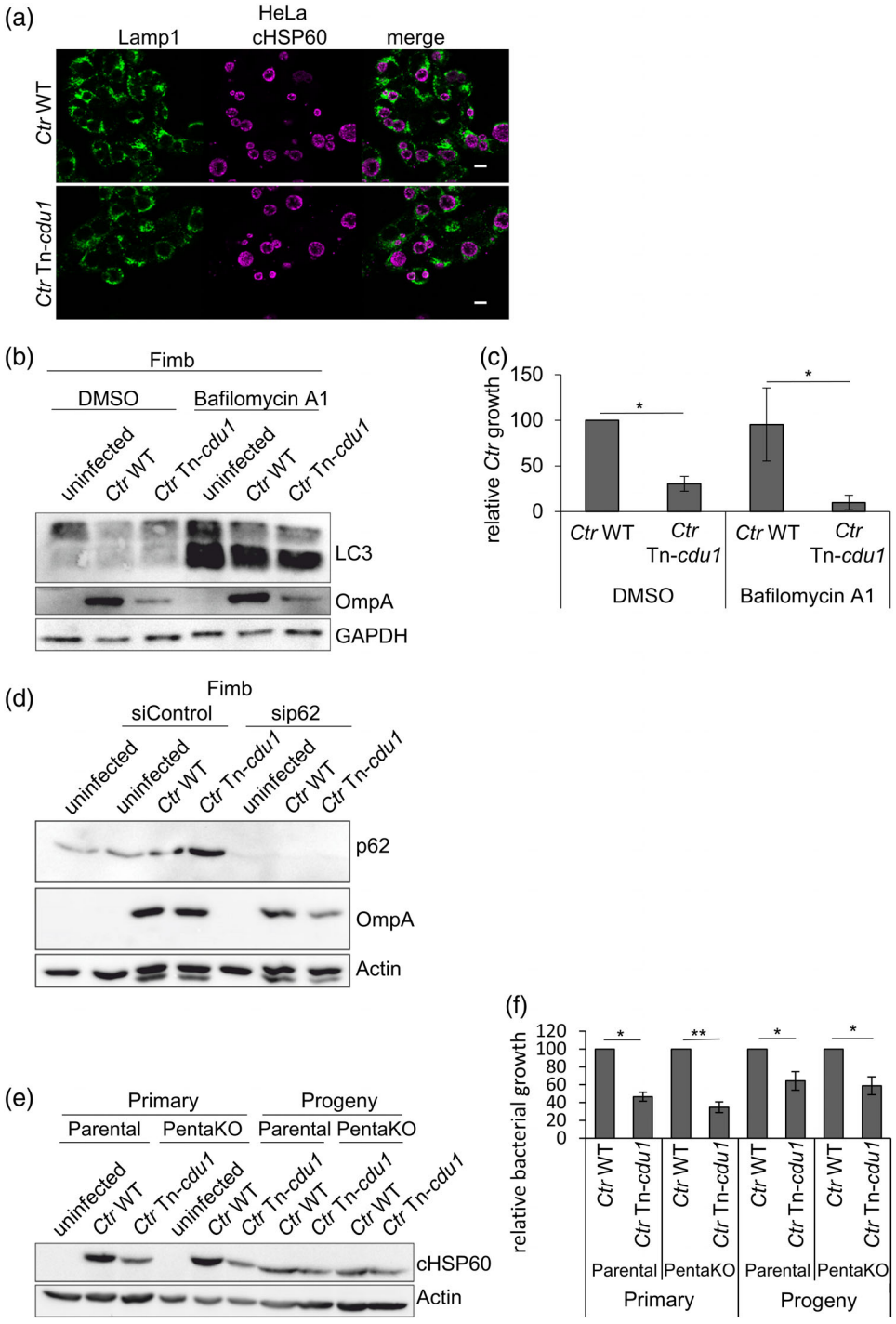

FIGURE 4 Growth and replication defect of *Ctr* Tn-*cdu1* in primary cells is independent of autophagy. (a) HeLa cells were infected with *Ctr* WT or *Ctr* Tn-*cdu1* at a MOI of 1 for 24 hr before cells were fixed with 4% PFA/sucrose. Cells were stained for Lamp1 (green) and cHSP60 (pink). Scale bar, 10 μm. (b) Primary Fimb cells were infected with *Ctr* WT or *Ctr* Tn-*cdu1* at a MOI of 0.3 for 24 hr and treated with or without 10 nM Bafilomycin A1 for 7 hr. Cells were lysed in SDS-sample buffer and immunoblot was performed. (c) Relative growth of *Ctr* WT and *Ctr* Tn-*cdu1* after 24 hr in Fimb cells treated with or without Bafilomycin A1 for 7 hr. Bacterial load was determined by quantifying chlamydial OmpA levels and normalisation to GAPDH (b). Significance was calculated using the Student's *t* test. * $p < .05$. (d) Fimb cells were treated with a control siRNA (siControl) or sip62 for 24 hr before infection with *Ctr* WT or *Ctr* Tn-*cdu1* at a MOI of 0.3. Lysates were taken 24 hpi and analysed by immunoblotting for p62, OmpA and actin. (e) Infectivity assay in PentaKO and Parental cells was performed. Cells were infected with *Ctr* WT and *Ctr* Tn-*cdu1* with a MOI of 1 and lysates from these primary infections were taken 24 hpi (Primary). For progeny infection cells were lysed 48 hpi and fresh HeLa cells were infected with the infections supernatant. Lysates for progeny infection were taken 24 hpi. Both, primary and progeny infection were analysed for chlamydial load by immunoblotting for cHSP60. (f) Quantification of immunoblots showing relative bacterial growth in PentaKO and Parental cells. Bacterial load was determined by quantifying chlamydial HSP60 (cHSP60) levels and normalisation to actin (e). Growth of wild-type *Chlamydia* was set to 100%. Results of three independent experiments are shown. Significance was calculated using the Student's *t* test. * $p < .05$, ** $p < .01$

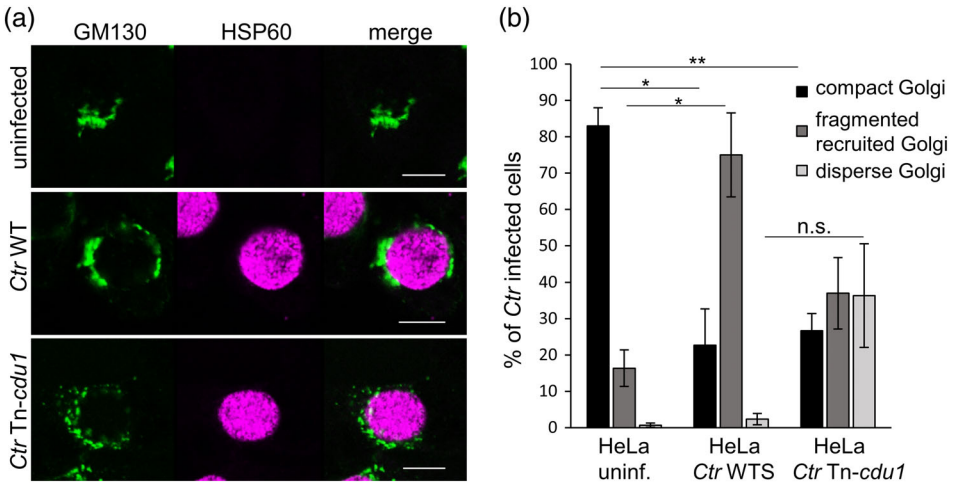

FIGURE 5 Altered Golgi recruitment in *Ctr* Tn-*cdu1* infected cells. (a) HeLa cells were left uninfected or were infected with *Ctr* WT or *Ctr* Tn-*cdu1* at a MOI of 1 for 24 hr. For indirect immunofluorescence cells were fixed with 4% PFA/sucrose. *Chlamydia* were stained for cHSP60 (pink) and the Golgi for GM130 (green). Scale bar, 10 μm. (b) Quantification of immunofluorescence pictures showing intact and compact Golgi, fragmented and recruited or fragmented and dispersed Golgi in cells infected with *Ctr* WT or *Ctr* Tn-*cdu1*. Phenotype of Golgi in infected cells was determined and counted in immunofluorescence pictures obtained in (a). Three independent experiments were performed and approximately 100 cells were counted. Significance was calculated using the Student's *t* test. n.s. not significant, $*p < .05$, $**p < .01$

side (Fischer et al., 2017). We tested whether the inactive Cdu1 protein alters the ubiquitination pattern in the host cell. Indeed the inclusion of *Ctr* Tn-*cdu1* was decorated with K48 and K63 linked ubiquitin chains in contrast to the wild-type strain that shows no ubiquitin signal (Figure 2a, b). Interestingly even though *Ctr* Tn-*cdu1* grew normally in HeLa cells, inclusions were similarly ubiquitinated as in primary Fimb cells in which the development of EBs was affected (Figure 2a, b). To demonstrate that Cdu1 is responsible for the removal of ubiquitin residues at the inclusion surface, *cdu1* was expressed under the control of a tetracycline-inducible promoter. Addition of anhydrotetracycline (AHT), a potent inducer of the tetracycline promoter, resulted in the expression of wild-type Cdu1 without the membrane spanning domain in the HeLa Cdu1-Flag cell cytoplasm and the removal of ubiquitin from the *Ctr* Tn-*cdu1* inclusion (Figure 2c, d). A similar effect was observed in primary Fimb upon transfection of the pEGFP-N1/Cdu1 construct (Figure S2a). To demonstrate that Cdu1 activity is required to remove ubiquitin from the inclusion surface a HeLa cell line with an inactive Cdu1-Flag (Cdu1 (C345A)) was generated (HeLa Cdu1(C345A)-Flag) (Figure S1c) and the same construct was transfected into primary Fimb cells. Induction of Cdu1(C345A)-Flag failed to deubiquitinate inclusions in HeLa (Figure 2d, S1a). Likewise, deubiquitination of the inclusion was not observed upon transfection of Fimb cells with pEGFP-N1/Cdu1ΔCD lacking the catalytic C-terminal domain (Figure S2b), demonstrating that the Cdu1 deubiquitinase activity is required for the removal of ubiquitin from chlamydial inclusions. We then asked if the Cdu1 activity to remove ubiquitin from *Ctr* Tn-*cdu1* inclusions can also be provided by the wild-type bacteria in co-infection experiments. Simultaneous infection of HeLa cells with *Ctr* WT and *Ctr* Tn-*cdu1* revealed that active Cdu1 in the inclusion membrane cannot deubiquitinate other inclusions in the same cell that are not in direct proximity to the protease (Figure S3a). However, at sites of contact a deubiquitination activity locally removes ubiquitin from the surface of the mutant inclusion (Figure 2e, S3b). Interestingly, inclusion with both, Cdu1 wild-type and mutant bacteria did not display ubiquitin on the inclusion surface (Figure S3c) demonstrating that wild-type *Chlamydia* can complement the deubiquitination defect of *Ctr* Tn-*cdu1* from inside the inclusion. We conclude from these results that the chlamydial inclusion is constantly ubiquitinated in the absence of Cdu1 and the high deubiquitinating activity of Cdu1 removes ubiquitin from the surface of the inclusion.

2.3 | The autophagy machinery is recruited to the ubiquitinated inclusion

Ubiquitination via lysine 48 is often a signal for protein degradation by the proteasome, whereas a linkage via K63 preferably induces autophagy (Hershko & Ciechanover, 1998; Olzmann & Chin, 2008; Vucic et al., 2011). Autophagy adapters like sequestosome1 (hereafter referred to as p62) bind to ubiquitin K63 and subsequently recruit autophagy initiation proteins like LC3. Compared to inclusions of wild-type bacteria, inclusions of *Ctr* Tn-*cdu1* contained high amounts of p62 visible as surface-associated ring structures on these inclusions (Figure 3a, c). Furthermore, p62 protein levels were upregulated in cells infected with *Ctr* Tn-*cdu1* starting around mid-phase of the developmental cycle (Figure 3d, e). In addition to p62, the autophagy receptors next to BRCA1 gene 1 protein (NBR1) and NDP52 were also identified at the chlamydial inclusion of *Ctr* Tn-*cdu1* infected HeLa and Fimb cells (Figure S4 a–d). Autophagy cargo proteins like p62 bind to ubiquitin and facilitate the recruitment of LC3 for phagophore formation. During *Ctr* Tn-*cdu1* infection, levels of non-lipidated LC3I and lipidated and active LC3II increased during the mid-stage of the cycle (Figure 3d, e) and accumulation of all LC3 variants (LC3A,

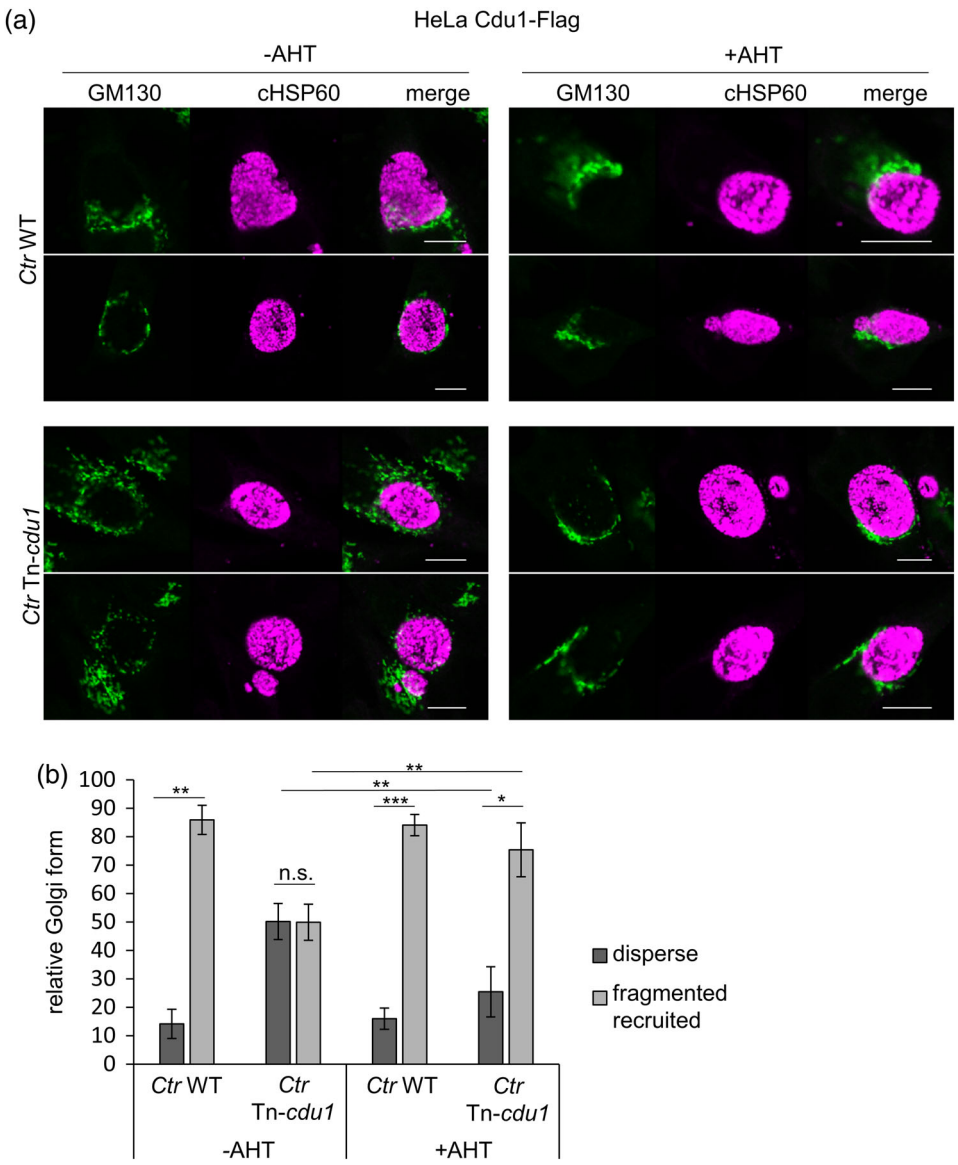

FIGURE 6 Altered Golgi recruitment in *Ctr* Tn-*cdu1* infected cells can be rescued. (a) HeLa FlpIn Cdu1Flag cells were infected with *Ctr* WT or *Ctr* Tn-*cdu1* at a MOI of 1 for 20 hr before 50 ng/ml AHT was added for 4 hr. For indirect immunofluorescence cells were fixed with 4% PFA/sucrose. *Chlamydia* were stained for cHSP60 (pink) and the Golgi for GM130 (green). Scale bar, 10 μm. (b) Quantification of immunofluorescence pictures showing fragmented recruited and fragmented dispersed Golgi in *Ctr* WT or *Ctr* Tn-*cdu1* infected HeLa cells. Phenotype of Golgi in infected cells was determined and counted in immunofluorescence pictures obtained in (a). Three independent experiments were performed and approximately 100 cells were counted. Significance was calculated using the Student's *t* test. n.s. not significant, $*p < .05$, $**p < .01$, $***p < .001$

LC3B, LC3C) (Figure S4 i–k) as well as the ATG8 family members GABARAP, GABARAPL1 and GABARAPL2 (Figure S4 f–h) were detected around the inclusion (Figure 3c, Figure S4 f–k) which indicates the formation of an autophagophore that was observed for the mutant but not the wild-type *Chlamydia* (Figure 3b, f). In addition the lipidation of LC3I to form lipidated LC3II initiating autophagophore formation depends on a multi-protein complex which also includes ATG12. ATG12 was also identified at the inclusion of *Ctr* Tn-*cdu1* (Figure S4e). These experiments confirmed the recruitment of autophagy receptors to and the formation of a LC3 positive double membrane around the inclusion of *Ctr* Tn-*cdu1* during infection.

2.4 | The growth defect of *Ctr* Tn-*cdu1* in primary cells is independent of autophagy

Phagophore formation and recruitment of the autophagy machinery to bacteria containing vacuoles are clear indications of active xenophagy. We therefore tested whether autophagosomes forming around the *Ctr* Tn-*cdu1* inclusion fuse with lysosomes. However, co-localization with the lysosomal marker protein Lamp1 could not be observed (Figure 4a). As the autophagy system is recruited to the inclusion we tested whether autophagy actively degrades the bacteria which would explain the observed growth defect of the mutant in primary cells. The lysosomal inhibitor Bafilomycin A1 interferes with the degradation of bacteria by inhibition of the H^+-ATPase and prevention of the acidification of the lysosomal lumen. To determine the bacterial load upon inhibitor treatment, levels of bacterial OmpA or HSP60 protein were detected by immunoblotting. These assays revealed that Bafilomycin A1 treatment could not rescue the growth defect in *Ctr* Tn-*cdu1* (Figure 4b, c). To further corroborate that reduced infectivity of the mutant depends on autophagy we also targeted the early stages of autophagy. Knock down of the key autophagy marker p62 in primary Fimb cells did not rescue the growth defect of *Ctr* Tn-*cdu1* (Figure 4d). Several different autophagy receptors in addition to p62 were identified at the inclusion of *Ctr* Tn-*cdu1* that could compensate

for reduced p62 levels. Therefore, a PentaKO cell line with deletions in the autophagy markers p62, NBR1, NDP52, Optineurin and TAX1BP1 was used to test the involvement of any known autophagy marker (Lazarou et al., 2015). The PentaKO cell line as well as the parental strain are also negative for Parkin E3 ligase. Knock out of all these autophagy genes did not rescue the growth of *Ctr* Tn-*cdu1* in primary or progeny infection (Figure 4e, f). In line with previous results we therefore claim that the growth defect of *Ctr* Tn-*cdu1* is not due to the autophagy and degradation by the lysosome but rather a slowed replication and transition of chlamydial RBs to EBs.

2.5 | Altered Golgi fragmentation of *Ctr* Tn-*cdu1* can be rescued

Reasons for impaired development in *Chlamydia* can be various. As obligate intracellular bacteria *Chlamydia* are known to consume metabolites and nutrients from the host cell. In wild-type *Chlamydia* infected cells the Golgi is fragmented and recruited to the inclusion surface for enhanced lipid acquisition by the bacteria (Heuer et al., 2009). In *Ctr* Tn-*cdu1* infected HeLa cells we find the Golgi also fragmented, however, recruitment to the chlamydial inclusion is impaired and the fragmented Golgi vesicle appeared dispersed around the inclusion (Figure 5a, b). To demonstrate that this reduced Golgi vesicle recruitment is due to a defect in Cdu1 activity in cells infected with mutant *Chlamydia* we expressed active Cdu1 in the cytoplasm of the cell. In cells complemented with Cdu1 Golgi stacks were recruited to the *Ctr* Tn-*cdu1* inclusion as in wild-type infected cells (Figure 6a, b). Golgi fragmentation was hardly visible in infected Fimb cells (Figure S5) suggesting that defects in Golgi fragmentation do not account for the growth difference of wild-type and mutant *Chlamydia* in these cells. Furthermore, acquisition of ceramide appeared neither affected in HeLa nor in Fimb cells (Figure S6), ruling out a defect in ceramide uptake as a reason for the developmental defect of *Ctr* Tn-*cdu1*. All in all our data suggest that Cdu1 is required for the efficient recruitment of Golgi vesicles to the inclusion surface of *Chlamydia*, an effect that appears to be host cell dependent and independent of ceramide uptake into the inclusion.

3 | DISCUSSION

Obligate intracellular bacteria like *Chlamydia* acquire metabolites from the host cell, which is expected to induce nutrient stress and autophagy. In addition, recent research into the role of autophagy as cell autonomous defence against intracellular pathogens suggested that autophagy not only defeats bacteria residing in the cytosol of the host but also bacteria in membrane bound phagosomes if these are leaky (Birmingham et al., 2006; Gomes & Dikic, 2014; Mitchell & Isberg, 2017). It was therefore an obvious assumption that autophagy may play a role in restricting chlamydial infection either as a consequence of nutrient stress or as cell autonomous defence. Our data suggest a complex interaction of *Chlamydia* with cell autonomous defence mechanisms restricting metabolite acquisition and autophagic destruction.

Although *Chlamydia* does not reside in the cytosol of host cells for extended times, a leaky or perforated inclusion membrane during late stage infections or as a consequence of cell autonomous immune attack may offer targets for activating autophagy (Fischer & Rudel, 2018; Weber et al., 2017a). In *Ctr* Tn-*cdu1*, but not in wild-type infected cells we find the inclusion decorated with ubiquitin and recruitment of autophagy proteins already during the replicative phase of the bacteria (24 hpi) when the inclusion is still intact (data not shown). We therefore postulate that the chlamydial inclusion is constantly targeted by the autophagy machinery but the chlamydial deubiquitinase Cdu1 efficiently interferes with this process at the initial steps by removing ubiquitin from the inclusion surface. This role of Cdu1 is supported by the observation that substitution of active Cdu1 in the cell cytoplasm removes the ubiquitin moieties from the inclusion membrane, emphasising the importance of the active DUB for keeping the inclusion free of ubiquitin (Figure 2c, d). In infected cells, this process is restricted to the inclusion surface where the deubiquitinase is anchored, since wild-type Cdu1 is not able to deubiquitinate neighbouring mutant inclusions; the involvement of soluble cytosolic factors can be excluded.

In contrast to our observations, LC3 has been shown to be recruited to *C. trachomatis* inclusions in other studies (Al-Younes et al., 2004; Al-Younes et al., 2011). These authors used a polyclonal goat antiserum (which is no longer available) which was directed against the unmodified LC3 form. It is therefore possible that the modified active LC3 preferably detected by the antibody used in this study is recruited only to the ubiquitinated inclusion. Despite the strong ubiquitination and the recruitment of autophagy receptors and effectors for phagophore formation to the inclusion in mutant infected cells, autophagy appears not to be a major mechanism by which host cells restrict chlamydial infection. Interestingly, p62 and LC3 are increased during the mid-phase of infection, when Cdu1 protein levels are also upregulated (Fischer et al., 2017). Since we neither find ubiquitination nor the recruitment of autophagy marker during the early phase of infection before Cdu1 is expressed, the inclusion may either not be detected or detection by the autophagic system may be actively prevented independent of Cdu1. Moreover, inhibition of autophagy neither in early phases by knock down of autophagy receptors (Figure 4d, e, f) nor in late phases by Bafilomycin A1 inhibitor treatment (Figure 4b, c) could rescue the growth defect of *Ctr* Tn-*cdu1*. Also inclusions of mutant *Chlamydia* in HeLa cells that do not restrict growth and progeny infection are also decorated with autophagy markers (Figures 2a and 3a, Figure S4a, b). Finally, no fusion with lysosomes was detected indicating that *Ctr* Tn-*cdu1* is not degraded in autolysosomes (Figure 4a). These findings therefore strongly suggest that the growth defect of *Ctr* Tn-*cdu1* is not due to clearance of infection by autophagy.

Our electron microscopic analyses revealed a reduced number of EBs in *Ctr* Tn-*cdu1* compared to wild-type bacteria (Figure 1c, d) in line with impaired progeny infection of the mutant. We therefore postulate that redifferentiation of RBs to EBs is affected in *Ctr* Tn-*cdu1*. Recently redifferentiation has been correlated to the RB size which is reduced in every replication cycle until a certain threshold is reached and EBs are formed (Lee et al., 2018). Analysis of bacterial RB size

demonstrated that mutant bacteria are larger (Figure 1e) consistent with a disturbed differentiation to EBs. Although the complete mechanism of RB to EB transition is still unknown, the observed phenotype could be explained by slowed growth and replication of *Ctr* Tn-*cdu1*. Since bacteria depend on host metabolites for growth that they also take from organelles like the Golgi apparatus, the structure of the Golgi was further analysed. Indeed, Golgi membranes were less recruited to the *Ctr* Tn-*cdu1* than the wild-type inclusions (Figure 5a, b). Reduced availability of Golgi membranes at the chlamydial inclusion is known to limit chlamydial growth (Heuer et al., 2009; Lipinski et al., 2009). However, we could not observe a major difference in the uptake of ceramide into the inclusion of wild-type *Chlamydia* and *Ctr* Tn-*cdu1*. Furthermore, the growth defect of *Ctr* Tn-*cdu1* was prominent in primary Fimb cells, which neither display major Golgi fragmentation upon infection with wild-type or mutant *Chlamydia* nor defects in ceramide uptake into their inclusions. Recently, *Ctr* Tn-*cdu1* was suggested to avoid Golgi fragmentation (Pruneda et al., 2018). In contrast to their data we did see Golgi fragmentation in the cytoplasm of *Ctr* Tn-*cdu1* infected cells but reduced association of Golgi vesicles with the inclusion. Recruitment of Golgi vesicles to the inclusion could be rescued by expression of active Cdu1 (Figure 6a, b) consistent with a central role of Cdu1 in this process. Although our data argue against a central role of Golgi fragmentation or Golgi vesicle recruitment to the inclusion as major reason for the growth defect of the Cdu1 mutant, Cdu1 appears to be a key factor required to keep the inclusion surface susceptible for interaction with host vesicular trafficking and possibly nutrient acquisition.

4 | EXPERIMENTAL PROCEDURES

4.1 | Cell lines and cultivation

HeLa 229 cells (ATCC Cat# CCL-2.1, RRID:CVCL_1276; tested negative for mycoplasma contamination by polymerase chain reaction (PCR)), primary Fimb cells (primary cells of human fimbriae obtained from biopsies of patients undergoing medically indicated surgery. According to the hospitalisation contract patients agreed to scientific use of biopsies after anonymization of samples; tested negative for mycoplasma contamination by PCR), U2OS cells expressing GFP (green fluorescent protein)-LC3 or GFP-GABARAP (kind gift of Alexandra Stolz) and PentaKO or Parental cells (kind gift of Michael Lazarou) were cultured in RPMI (Roswell Park Memorial Institute)-1640 medium (Gibco, Waltham, MA) supplied with 10% fetal calf serum (FCS) (Paa, Germany). HUVEC (ATCC Cat# CRL-1730; tested negative for mycoplasma contamination by PCR) were grown in medium 200 supplemented with low serum growth supplement (Thermo Fischer, Waltham, MA). Cells were cultivated by 37°C and 5% CO_2. HeLa Cdu1-Flag inducible cell line was obtained by transfection of FlpIn HeLa (kind gift of Ivan Dikic) cells with pcDNA5FRT/Cdu1deltaTM-Flag plasmid and selection with hygromycin. The pcDNA5FRT/Cdu1deltaTM-Flag plasmid was obtained by PCR using the forward primer GATCGATATCATGTTATCTCCCACCAACTCA and the reverse primer GATCGCGGCCGCTTACTTATCGTCGTCATCCTT GTAATCTGCTTCAGGCCAAGAAAGCT and genomic DNA of *Chlamydia trachomatis* L2 strain 434/Bu as template. Gene expression was initiated by addition of 50 ng/ml AHT.

4.2 | siRNA knock-down in Fimb cells

For the siRNA knock-down Fimb cells were seeded in 12-well plates and incubated over night at 37°C and 5% CO_2. For transfection siRNA was diluted in 50 µl OptiMEM to a concentration of 300 nM and incubated for 5 min. From the transfection reagent Lipofectamine RNAiMAX 0.8 µl per well was mixed with 50 µl OptiMEM and incubated at room temperature for 5 min. The siRNA mixture and the transfection reagent was mixed and incubated at room temperature for another 20 min. Supernatant was removed from the cells and overlayed with 5% FCS RPMI 1640 medium. The siRNA Lipofectamine mixture was added to the cells to a final concentration of siRNA of 30 nM. After 7 hr the medium was exchanged with fresh 20% FCS RPMI 1640 medium. Two days later the transfected cells were infected with *Ctr* Tn-*cdu1* or *Ctr* WT with an MOI of 0.3.

4.3 | Cultivation of *Ctr* and inhibitor treatment

For chlamydial infection cells were grown until a confluency of 70% was reached. Medium was exchanged for RPMI-1640 containing 5% FCS and chlamydial particles resembling a MOI of 1. Cells were incubated at 35°C and 5% CO_2 until further needed. For inhibitor treatment 10 nM Bafilomycin A1 (Thermo Fischer) or 2 µM MLN4924 was added to the infected cells 17 or 22 hpi respectively. For stock preparation cells were scraped and lysed with glass beads 48 hpi. *Chlamydia* were separated by centrifugation at 1000*g* for 10 min and pelleted at 30 000*g* for 30 min both at 4°C. After washing the bacteria with 1× sucrose-phosphate-glutamic acid (SPG buffer (75 g/L sucrose, 0.52 g/L KH_2PO_4, 1.22 g/L Na_2HPO_4, 0.72 g/L L-glutamic acid, pH 7.4) *Chlamydia* were re-suspended in 1× SPG, aliquoted and stored at −80°C until needed. Bacteria were tested for mycoplasma contamination by PCR and inclusion forming unit was determined.

4.4 | Infectivity assays

Fimb, HUVEC HeLa and PentaKO cells were seeded in two 12 well microplates and grown to a confluency of 70%. Cells were infected with *Ctr* WT or *Ctr* Tn-cdu1 with an MOI of 1 for HeLa and PentaKO cells and an MOI of 0.3 for primary cells as described before. Primary lysates were taken 24 hpi by adding 2× SDS lysis buffer (100 mM Tris/HCl [pH 6.8], 20% glycerin, 4% SDS, 1.5% 2-mercaptoethanol, 0.2% bromphenolblue) to the cells. For progeny infection infected cells were lysed with glass beads 48 hpi and an aliquot of the supernatant was used to infect a fresh 12 well plate seeded with fresh cells. Lysates of progeny infection were taken 24 hpi as described. For analysis in immunoblot lysates were heated at 94°C for 5 min.

4.5 | Indirect immunofluorescence

Cells were grown on glass cover slides and infected as described above. For inducible cell lines 50 ng/ml AHT was added 4 hr before harvest. Cells were washed with phosphate-buffered saline (PBS) (Gibco) once and fixed using 4% PFA/sucrose. After permeabilisation with 0.2% TritonX 100 in PBS for 30 min, antigens were blocked with 2% FCS in PBS for 1 hr. Primary antibodies were diluted as follows in 2% FCS in PBS: anti-K48 (Merck #05-1,307, 1:500), anti-K63 (Merck #05–1,308, 1:100), anti-Ubi FK2 (Enzo #BML-PW8810-0500, 1:200), anti-cHSP60 (selfmade, 1:800), anti-Cdu1 (selfmade (Fischer et al., 2017), 1:300), anti-p62 (santa cruz #sc-28,359, 1:1000), anti-LC3B (cell signalling #2775, 1:50), anti-NBR1 (santa cruz #sc-130,380, 1:200), anti-NDP52 (santa cruz #sc-376,540, 1:200), anti-ATG12 (cell signalling #2010, 1:200), anti-Ankib1 (Thermo Fischer #PA5-54506, 1:200), anti-GM130 (BD #610823, 1:400), anti-Lamp1 (santa cruz #sc-18,821, 1:200). After incubation with the primary antibody for 1 hr at room temperature, remaining antibody was washed away and the secondary Cy3 or Cy5 coupled antibody (Dianova) was diluted 1:300 in 2% FCS in PBS and incubated in the dark for 1 hr. Nucleic acid was stained with DAPI for 30 min.

4.6 | Ceramide uptake assay by live cell imaging

Cells were seeded in glass bottom dishes (ibidi, Gräfelfing, Germany) and infected with *Ctr* WT and *Ctr* Tn-*cdu1* for 24 hr. 1.5 μM SiR-DNA dye (Spirochrome, Stein am Rhein, Switzerland) was added and incubated for 1 hr. Cells were washed three times with PBS, before live cell imaging media (RPMI 1640 (Gibco) + 25 mM N-2-hydroxyethylpiperazine-N-2-ethane sulfonic acid (HEPES) (Gibco)) was added. Imaging was performed using a Leica TCS SP5 confocal microscope with a 63× oil immersion objective connected with a prewarmed (37°C) incubation chamber. 0.5 μM nitrobenzoxadiazole (NBD)-C_6-ceramide (Invitrogen, Waltham, Massachusetts, USA) was added to the cells and images were acquired every minute using the LAS software. Recorded pictures were processed with ImageJ.

4.7 | Immunoblotting

Lysates were loaded on a 10% SDS PAGE and transferred on a PVDF membrane (Roche, Basel, Switzerland) using the semidry blotter (Thermo Fischer). Membranes were blocked in 5% bovine serum albumin/tris-buffered saline (BSA/TBS) containing 0.05% Tween20 (TBS-T) or 5% milk/TBS-T for 1 hr and incubated with the primary antibody diluted in 5% BSA/TBS-T or 5% milk/TBS-T at 4°C overnight. Primary antibodies were diluted as follows: anti-LC3B (cell signalling #2775, 1:500), anti-HSP60 (santa cruz #sc-57,840, 1:1000), anti-Actin (Sigma Aldrich #A5441, 1:1000), anti-p62 (santa cruz #sc-28,359, 1:1000), anti-OmpA (selfmade, 1:1000), anti-GAPDH (santa cruz, #sc-25,778, 1:1000). After incubation membranes were washed three times with TBS-T and incubated with the secondary antibody in 5% milk/TBS-T for 1 hr at room temperature. The anti-mouse-horseradish peroxidase (HRP) (santa cruz, #sc-516102) and anti-rabbit-HRP (Dianova, #111-035-144) secondary antibodies were diluted 1:3000. Blots were washed as described and analysed using ECL solutions and the Intas Chem HR 16–3200 reader. Blots were quantified using ImageJ software.

4.8 | Transmission electron microscopy

Fimb cells were seeded on glass cover slides and infected with *Ctr* Tn-*cdu1* or *Ctr* WT with an MOI of 1. After 24 or 30 hr of infection slides were washed once with PBS and fixed using 2.5% glutaraldehyde in 0.05 M Cacodylate buffer for 30 min at room temperature. Cells were washed in Cacodylate buffer, incubated in 2% OsO_4/0.05 M Cacodylate buffer for 1 hr and in 0.5% Uranylacetat overnight. Samples were dehydrated and embedded in EPON and cut. Images were taken with the JEOL JEM-2100 microscope. For analysis of RB diameter pictures were measured in ImageJ with five inclusions per sample.

4.9 | Statistical analysis

Statistical analysis was performed using Excel. Statistical significance between groups was determined using two-tailed Student's *t* test. Data are shown as mean ± *SE*.

ACKNOWLEDGMENTS

We thank Michael Lazarou for the PentaKO and Parental cell lines and Ivan Dikic and Alexandra Stolz for the FlpIn HeLa cells and U2OS cells. We thank Daniela Bunsen and Claudia Gehrig for support of sample preparation for EM. We thank Andreas Demuth for editing the manuscript. This work was supported by the Deutsche Forschungsgemeinschaft (DFG) GRK 2243 "Understanding Ubiquitylation: From Molecular Mechanisms to Disease" to T.R. This publication was funded by the German Research Foundation (DFG) and the University of Wuerzburg in the funding programme Open Access Publishing.

CONFLICT OF INTEREST

The authors declare that they have no conflict of interest with the contents of this article.

ORCID

Thomas Rudel https://orcid.org/0000-0003-4740-6991

REFERENCES

Al-Younes, H. M., Al-Zeer, M. A., Khalil, H., Gussmann, J., Karlas, A., Machuy, N., … Meyer, T. F. (2011). Autophagy-independent function of MAP-LC3 during intracellular propagation of *Chlamydia trachomatis*. *Autophagy*, *7*, 814–828.

Al-Younes, H. M., Brinkmann, V., & Meyer, T. F. (2004). Interaction of *Chlamydia trachomatis* serovar L2 with the host autophagic pathway. *Infection and Immunity*, *72*, 4751–4762.

Bartlett, E. C., Levison, W. B., & Munday, P. E. (2013). Pelvic inflammatory disease. *BMJ: British Medical Journal*, *346*, f3189.

Bébéar, C., & de Barbeyrac, B. (2009). Genital *Chlamydia trachomatis* infections. *Clinical Microbiology and Infection*, *15*, 4–10.

Birmingham, C. L., Smith, A. C., Bakowski, M. A., Yoshimori, T., & Brumell, J. H. (2006). Autophagy controls Salmonella infection in response to damage to the Salmonella-containing vacuole. *Journal of Biological Chemistry*, *281*, 11374–11383.

Dikic, I. (2017). Proteasomal and autophagic degradation systems. *Annual Review of Biochemistry*, *86*, 193–224.

Engel, J. (2004). Tarp and Arp: How Chlamydia induces its own entry. *Proceedings of the National Academy of Sciences*, *101*, 9947–9948.

Fischer, A., Harrison, K. S., Ramirez, Y., Auer, D., Chowdhury, S. R., Prusty, B. K., … Rudel, T. (2017). *Chlamydia trachomatis*-containing vacuole serves as deubiquitination platform to stabilize Mcl-1 and to interfere with host defense. *eLife*, *6*, e21465.

Fischer, A. and Rudel, T. (2016). *Subversion of cell-autonomous host defense by Chlamydia infection*. In Häcker, G. (Ed.), Biology of Chlamydia. Current Topics in Microbiology and Immunology, vol 412. Cham: Springer.

Fischer, A., & Rudel, T. (2018). Safe haven under constant attack—The Chlamydia-containing vacuole. *Cellular Microbiology*, *20*, e12940.

Geisler, S., Holmström, K. M., Skujat, D., Fiesel, F. C., Rothfuss, O. C., Kahle, P. J., & Springer, W. (2010). PINK1/Parkin-mediated mitophagy is dependent on VDAC1 and p62/SQSTM1. *Nature Cell Biology*, *12*, 119–131.

Gomes, L. C., & Dikic, I. (2014). Autophagy in antimicrobial immunity. *Molecular Cell*, *54*, 224–233.

Hackstadt, T., Rockey, D. D., Heinzen, R. A., & Scidmore, M. A. (1996). *Chlamydia trachomatis* interrupts an exocytic pathway to acquire endogenously synthesized sphingomyelin in transit from the Golgi apparatus to the plasma membrane. *The EMBO Journal*, *15*, 964–977.

Haldar, A. K., Piro, A. S., Finethy, R., Espenschied, S. T., Brown, H. E., Giebel, A. M., … Coers, J. (2016). *Chlamydia trachomatis* is resistant to inclusion ubiquitination and associated host defense in gamma interferon-primed human epithelial cells. *MBio*, *7*, e01417-16.

Hershko, A., & Ciechanover, A. (1998). The ubiquitin system. *Annual Review of Biochemistry*, *67*, 425–479.

Heuer, D., Lipinski, A. R., Machuy, N., Karlas, A., Wehrens, A., Siedler, F., … Meyer, T. F. (2009). Chlamydia causes fragmentation of the Golgi compartment to ensure reproduction. *Nature*, *457*, 731–735.

Huibregtse, J., & Rohde, J. R. (2014). Hell's BELs: Bacterial E3 ligases that exploit the eukaryotic ubiquitin machinery. *PLoS Pathogens*, *10*, e1004255.

Hybiske, K., & Stephens, R. S. (2007). Mechanisms of host cell exit by the intracellular bacterium Chlamydia. *Proceedings of the National Academy of Sciences of the United States of America*, *104*, 11430–11435.

Kimmelman, A. C. (2011). The dynamic nature of autophagy in cancer. *Genes & Development*, *25*, 1999–2010.

Kirkin, V., Lamark, T., Johansen, T., & Dikic, I. (2009). NBR1 co-operates with p62 in selective autophagy of ubiquitinated targets. *Autophagy*, *5*, 732–733.

Kleiger, G., & Mayor, T. (2014). Perilous journey: A tour of the ubiquitin–proteasome system. *Trends in Cell Biology*, *24*, 352–359.

Kreibich, S., Emmenlauer, M., Fredlund, J., Rämö, P., Münz, C., Dehio, C., … Hardt, W. D. (2015). Autophagy proteins promote repair of endosomal membranes damaged by the Salmonella type three secretion system 1. *Cell Host & Microbe*, *18*, 527–537.

Lazarou, M., Sliter, D. A., Kane, L. A., Sarraf, S. A., Wang, C., Burman, J. L., … Youle, R. J. (2015). The ubiquitin kinase PINK1 recruits autophagy receptors to induce mitophagy. *Nature*, *524*, 309–314.

Lee, J. K., Enciso, G. A., Boassa, D., Chander, C. N., Lou, T. H., Pairawan, S. S., … Tan, M. (2018). Replication-dependent size reduction precedes differentiation in *Chlamydia trachomatis*. *Nature Communications*, *9*, 45.

Lipinski, A. R., Heymann, J., Meissner, C., Karlas, A., Brinkmann, V., Meyer, T. F., & Heuer, D. (2009). Rab6 and Rab11 regulate *Chlamydia trachomatis* development and golgin-84-dependent Golgi fragmentation. *PLoS Pathogens*, *5*, e1000615.

Misaghi, S., Balsara, Z. R., Catic, A., Spooner, E., Ploegh, H. L., & Starnbach, M. N. (2006). *Chlamydia trachomatis*-derived deubiquitinating enzymes in mammalian cells during infection. *Molecular Microbiology*, *61*, 142–150.

Mitchell, G., & Isberg, R. R. (2017). Innate immunity to intracellular pathogens: Balancing microbial elimination and inflammation. *Cell Host & Microbe*, *22*, 166–175.

Newman, L., Rowley, J., Vander Hoorn, S., Wijesooriya, N. S., Unemo, M., Low, N., … Temmerman, M. (2015). Global estimates of the prevalence and incidence of four curable sexually transmitted infections in 2012 based on systematic review and global reporting. *PLoS One*, *10*, e0143304.

Olzmann, J. A., & Chin, L.-S. (2008). Parkin-mediated K63-linked polyubiquitination: A signal for targeting misfolded proteins to the aggresome-autophagy pathway. *Autophagy*, *4*, 85–87.

Pruneda, J. N., Bastidas, R. J., Bertsoulaki, E., Swatek, K. N., Santhanam, B., Clague, M. J., … Komander, D. (2018). A Chlamydia effector combining deubiquitination and acetylation activities induces Golgi fragmentation. *Nature Microbiology*, *1*, 1377–1384.

Subtil, A., Delevoye, C., Balañá, M.-E., Tastevin, L., Perrinet, S., & Dautry-Varsat, A. (2005). A directed screen for chlamydial proteins secreted by a type III mechanism identifies a translocated protein and numerous other new candidates. *Molecular Microbiology*, *56*, 1636–1647.

Svenning, S., & Johansen, T. (2013). Selective autophagy. *Essays in Biochemistry*, *55*, 79–92.

Thurston, T. L., Wandel, M. P., von Muhlinen, N., Foeglein, Á., & Randow, F. (2012). Galectin 8 targets damaged vesicles for autophagy to defend cells against bacterial invasion. *Nature*, *482*, 414–418.

Valdivia, R. H. (2008). Chlamydia effector proteins and new insights into chlamydial cellular microbiology. *Current Opinion in Microbiology*, *11*, 53–59.

Van Wijk, S. J., Fiskin, E., Putyrski, M., Pampaloni, F., Hou, J., Wild, P., … Dikic, I. (2012). Fluorescence-based sensors to monitor localization and functions of linear and K63-linked ubiquitin chains in cells. *Molecular Cell*, *47*, 797–809.

Vucic, D., Dixit, V. M., & Wertz, I. E. (2011). Ubiquitylation in apoptosis: A post-translational modification at the edge of life and death. *Nature Reviews Molecular Cell Biology*, *12*, 439–452.

Weber, M. M., Lam, J. L., Dooley, C. A., Noriea, N. F., Hansen, B. T., Hoyt, F. H., … Hackstadt, T. (2017a). Absence of specific *Chlamydia trachomatis* inclusion membrane proteins triggers premature inclusion membrane lysis and host cell death. *Cell Reports*, *19*, 1406–1417.

Wright, H. R., Turner, A., & Taylor, H. R. (2008). Trachoma. *The Lancet*, *371*, 1945–1954.

Yasir, M., Pachikara, N. D., Bao, X., Pan, Z., & Fan, H. (2011). Regulation of chlamydial infection by host autophagy and vacuolar ATPase-bearing organelles. *Infection and Immunity*, *79*, 4019–4028.

Zhang, Y., Higashide, W. M., McCormick, B. A., Chen, J., & Zhou, D. (2006). The inflammation-associated Salmonella SopA is a HECT-like E3 ubiquitin ligase. *Molecular Microbiology*, *62*, 786–793.

SUPPORTING INFORMATION

Additional supporting information may be found online in the Supporting Information section at the end of this article.

How to cite this article: Auer D, Hügelschäffer SD, Fischer AB, Rudel T. The chlamydial deubiquitinase Cdu1 supports recruitment of Golgi vesicles to the inclusion. *Cellular Microbiology*. 2020;22:e13136. https://doi.org/10.1111/cmi.13136